

# Correlation between flux pinning and inhomogeneous electronic distribution of $\text{Bi}_2\text{Sr}_2\text{CaCu}_2\text{O}_{8+\delta}$ directly probed by scanning tunneling microscopy/spectroscopy

Noritaka Fukuo, Hideki Mashima, and Yuji Matsumoto

*Materials and Structures Laboratory, Tokyo Institute of Technology, 4529 Nagatsutacho, Midori-ku, Yokohama 226-8503, Japan*

Taro Hitosugi and Tetsuya Hasegawa

*Department of Chemistry, University of Tokyo, 7-3-1 Hongo, Bunkyo-ku, Tokyo 113-0033, Japan*

(Received 17 April 2006; published 28 June 2006)

The correlation between the vortex distribution and electronic inhomogeneity in  $\text{Bi}_2\text{Sr}_2\text{CaCu}_2\text{O}_{8+\delta}$  single crystals has been studied by scanning tunneling microscopy/spectroscopy at 4.3 K under 8 T. Vortices have been visualized by mapping the differential tunneling conductance at 12.5 meV, at which quasiparticles form a bound state. We found that vortices tend to form a triangular lattice with a spacing of  $a_0=1.07(\phi_0/B)^{1/2}$  within a short range of  $\sim a_0$ , but that the triangular correlation is absent at longer ranges. By comparing the vortex distribution pattern and the spatial map of the gap value, we conclude that the vortices are predominantly trapped in the regions displaying relatively large gaps and rounded gap edges.

DOI: [10.1103/PhysRevB.73.220505](https://doi.org/10.1103/PhysRevB.73.220505)

PACS number(s): 74.50.+r, 74.72.Hs, 68.37.Ef, 74.25.Qt

Scanning tunneling microscopy/spectroscopy (STM/STS) is a powerful tool that enables us to directly visualize vortices trapped in high temperature superconductors (HTSCs) under an intense magnetic field. It does this by probing quasiparticle bound states around vortex cores, located at  $\sim \pm 5$  meV (Refs. 1 and 2) for  $\text{YBa}_2\text{Cu}_3\text{O}_{7-\delta}$  (YBCO) and  $\pm 6-9$  meV (Refs. 3-5) for  $\text{Bi}_2\text{Sr}_2\text{CaCu}_2\text{O}_{8+\delta}$  (Bi2212). In case of YBCO, vortices observed by STM/STS are arranged in an oblique lattice,<sup>1</sup> which is consistent with the results of small angle neutron scattering studies.<sup>6</sup> By contrast, the vortex distribution in Bi2212 was found to be considerably more disordered,<sup>3,7,8</sup> with the exception of one report<sup>5</sup> that proposed that vortices locally form a square lattice, whose primitive vectors are directed along the  $a$  and  $b$  axes.

It is generally believed that in HTSCs nanometer-scale structures effectively pin down vortices, because of their extremely short coherent lengths. Scanning tunneling microscopy/spectroscopy has been utilized to investigate the electronic nature of such structures to find possible candidates of effective pinning centers in HTSCs. These are classified into point defects,<sup>3,9-12</sup> such as oxygen vacancies and impurities in the  $\text{CuO}_2$  plane, planar-type defects,<sup>2,13,14</sup> including twin boundaries and phase separation boundaries, fine precipitates,<sup>15,16</sup> and radiation-induced columnar defects.<sup>17</sup> Recent STM/STS studies highlighted another nanoscale structure, electronic inhomogeneity inherent to Bi-based HTSCs, in which nanoscale domains indicating superconducting and pseudogaplike spectra coexist even at temperatures below  $T_c$ .<sup>18-24</sup> In the regions indicating pseudo-gaplike features, Zn impurities substituted for the Cu sites do not provide quasiparticle resonant states, clearly proving that the regions lack superconducting phase coherence.<sup>18</sup> This finding suggests that the nonsuperconducting regions, finely dispersed in a superconducting matrix, might act as strong pinning centers.<sup>23</sup> However, the correlation between vortex and electronic inhomogeneity has not been directly examined yet.

In this study, we have performed low temperature STM/STS measurements of  $\text{Bi}_2\text{Sr}_2\text{CaCu}_2\text{O}_{8+\delta}$  (Bi2212) under a

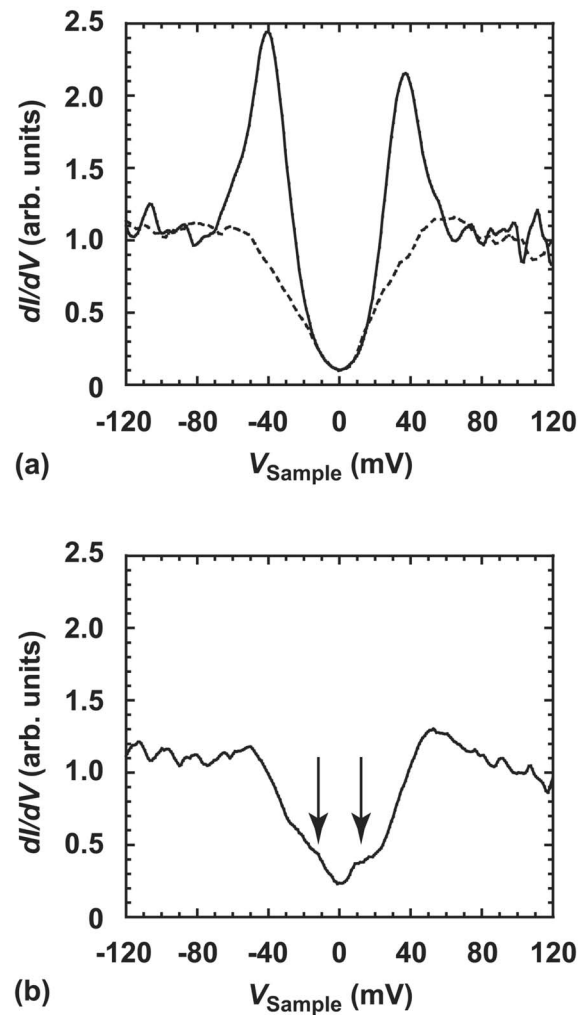


FIG. 1. (a) Typical tunneling spectra obtained at a location far from vortex cores and (b) inside a vortex core at 4.3 K under 8 T. The spectra are normalized at 100 mV. The bias voltage and set-point current are 200 mV and 0.2 nA, respectively.

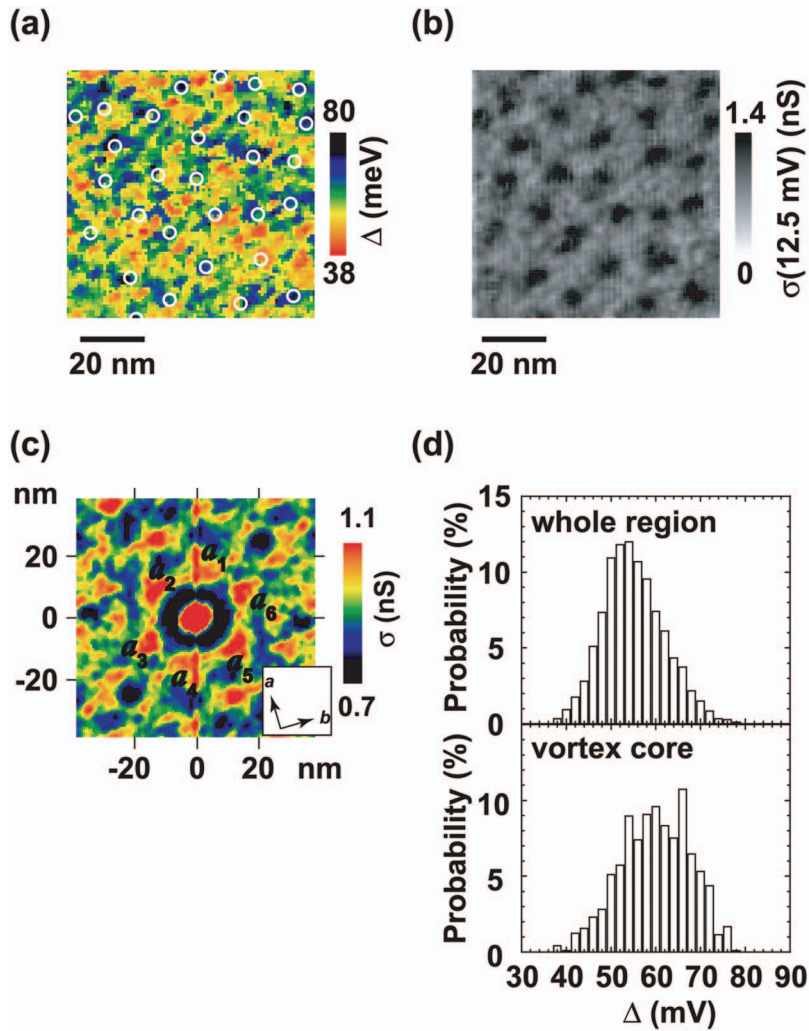


FIG. 2. (Color) STS results of Bi2212 single crystal at 4.3 K under 8 T. (a)  $\Delta$  map and (b) corresponding differential conductance image at 12.5 mV. The image size is  $77 \times 77 \text{ nm}^2$ . Circles in (a) indicate the locations of vortex cores. (c) Autocorrelation function calculated from (b). (d)  $\Delta$  distribution profiles derived from (a).

magnetic field of 8 T, in order to simultaneously observe both the vortex distribution and the electronic inhomogeneity. The comparison of the vortex images and the gap maps clearly demonstrates that vortices are predominantly trapped in the regions characterized by pseudogaps.

Bi2212 single crystals having a nominal composition of  $\text{Bi}_{2.1}\text{Sr}_{1.9}\text{CaCu}_{2.0}\text{O}_{8+\delta}$  were grown by the floating zone method. The superconducting transition temperature ( $T_c$ ) was determined to be 90 K (onset), using a SQUID suscep-

tometer. Scanning tunneling microscopy/spectroscopy measurements were carried out with a home-built ultrahigh vacuum, low temperature STM (UHV-LT-STM) instrument equipped with a low temperature cleavage stage. The base pressure of the STM chamber was maintained at less than  $2.0 \times 10^{-10}$  Torr during the measurements. All Bi2212 single crystals that were examined were cleaved *in situ* at 77 K, and then field-cooled to 4.2 K under a magnetic field of 8 T. The magnetic field was applied perpendicular to the sample sur-

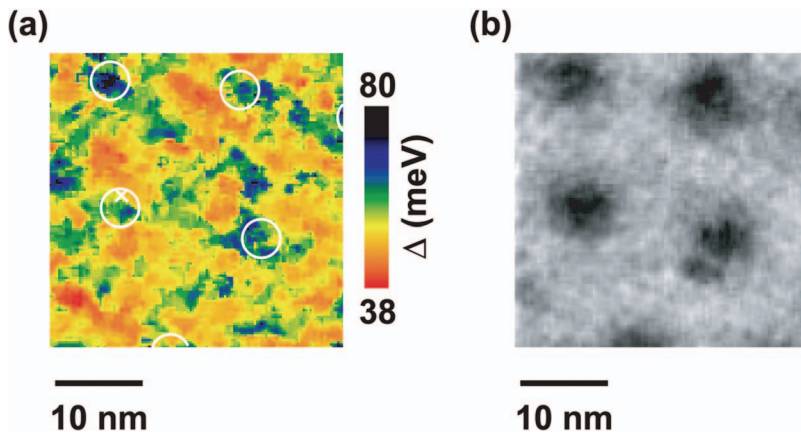


FIG. 3. (Color) (a)  $\Delta$  map and (b) corresponding differential conductance image at 12.5 mV. These images were obtained at 4.3 K under 8 T. The image size is  $30 \times 30 \text{ nm}^2$ . Circles in (a) indicate the locations of vortex cores.

face. Mechanically sharpened Pt-Ir wires were used as STM tips.

In order to investigate the vortex pinning associated with electronic inhomogeneity, we wanted to compare vortex images taken under a magnetic field with a  $\Delta$  map of the same region acquired without an external field. However, this is difficult to do experimentally, because of the considerable thermal drifting that occurs during the field-cooling process and/or mechanical deformation under intense magnetic field. Instead, we investigated the correlation between vortex and  $\Delta$  maps under a magnetic field of 8 T. Figure 1(a) plots typical tunneling spectra acquired under 8 T at 4.3 K, indicating superconducting (solid line) and pseudogap (dotted line) features. Superconducting gaps are characterized by a relatively small  $\Delta$ ,  $\Delta=40\text{--}60$  meV, and sharp coherence peaks, while pseudogaps are characterized by a larger gap of  $\geq 60$  meV with rounded gap edges. Figure 2(a) is a spatial map of  $\Delta$ , defined as half the peak-to-peak separation. The figure clearly indicates spatial variation of  $\Delta$  on a scale of several nanometers. The average and the standard deviations of  $\Delta$  are estimated to be  $\bar{\Delta}=56.0$  meV and  $\delta\Delta=6.8$  meV, respectively. As the origin of the electronic inhomogeneity, an unscreened Coulomb potential associated with excess oxygen atoms in the  $(\text{BiO})_2$  layers has been argued from both experimental and theoretical viewpoints.<sup>25</sup>

It has been reported that tunneling spectra in the vortex cores of Bi2212 show small peak structures inside the main gap, which, it has been argued, are the lowest excitation states of quasiparticles bound to the vortex cores, even though their locations differ slightly from one report to another.<sup>3–5,8</sup> We also observed such structures at  $\pm 12.5$  meV, as indicated by arrows in Fig. 1(b). Thus, we mapped the differential tunneling conductance at  $+12.5$  meV,  $\sigma(12.5$  meV), to visualize the vortex cores. The resulting  $\sigma(12.5$  meV) map, measured over the same region as Fig. 2(a), is shown in Fig. 2(b), where the dark regions represent vortex cores. Notably, Fig. 2(b) exhibits a local triangular lattice, which is substantially disordered in the whole observation area of Fig. 2(b). Figure 2(c) is an auto-correlation function calculated from Fig. 2(b). Six peaks with hexagonal symmetry, labeled as  $\mathbf{a}_i$  ( $i=1\text{--}6$ ), are recognizable near the origin, but the nearest neighbor peaks, which should be located at  $\mathbf{a}_{i+j}$ , are absent. A broad peak structure near  $\mathbf{a}_1+\mathbf{a}_2$  was not reproducible from one measurement to another. The average distance between the origin and  $\mathbf{a}_i$  is 17.4 nm, which is very close to the value anticipated in an ideal triangular vortex lattice under 8 T,  $a_0=1.07(\phi_0/B)^{1/2}=17.3$  nm. These facts indicate that vortices tend to form a triangular lattice within a short distance from  $a_0$ , but the triangular correlation disappears over a longer range  $>a_0$ . The local vortex lattice is not related to the crystallographic axes, as shown in Fig. 2(c), in contrast with the work by Matsuba *et al.* reporting alignment of vortices along the  $a$  or  $b$  axis.<sup>5</sup> However, we cannot exclude the possibility that an orientational order of vortices exists throughout the sample due to vortex alignment along a specific crystallographic axis, as reported by techniques which obtain information averaged over the entire samples, such as neutron scattering.<sup>26</sup>

Next, we discuss the correlation between the gap inhomogeneity and the vortex distribution.

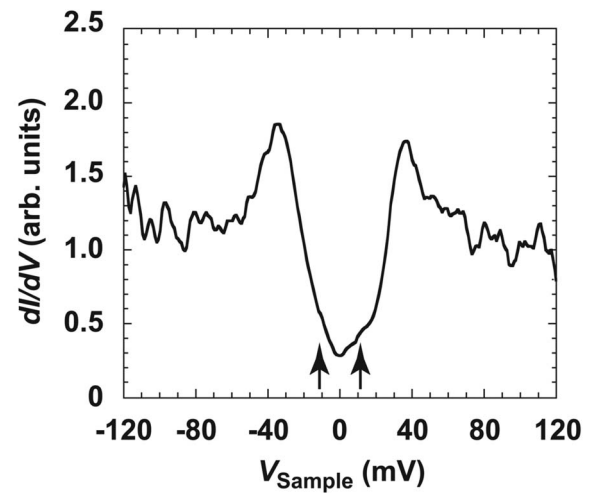


FIG. 4. Tunneling spectrum measured at the location marked by a cross in Fig. 3(a). Arrows indicate the structures at  $\pm 12.5$  meV.

As shown in Fig. 2(a), we define vortex cores as circular regions with a coherence length radius of  $\xi=1.9$  nm, which is evaluated as the full width at half maximum (FWHM) of the cross-sectional  $\sigma$  (12.5 meV) profiles across vortices. There is a clear tendency for the vortices to be located in the regions having larger  $\Delta$ . This is seen more clearly in Fig. 2(d), which compares the  $\Delta$  distribution histograms evaluated from the whole area of Fig. 2(a) and the vortex core regions surrounded by circles. Inside the vortex cores, the distribution profile shifts to higher energies. In Fig. 2(a), some vortices seem to exist in the low  $\Delta$  regions. However, higher resolution measurements confirmed that all vortices observed in Fig. 2(a) are trapped by the high- $\Delta$  regions. Figures 3(a) and 3(b) show higher resolution  $\Delta$  and  $\sigma$  (12.5 meV) maps, respectively, observed from a different spatial location from that of Fig. 2. Again, vortices occupy the high- $\Delta$  regions.

The above-mentioned behavior can be interpreted in two different ways. One interpretation is that the vortices destroy superconductivity and induce pseudogap states around the vortex cores. The other assumes that vortices prefer to penetrate the high- $\Delta$  regions originally incorporated in the crystal because they gain condensation energy. If the first interpretation is correct, the vortex cores should always exhibit pseudogaplike spectra with larger values of  $\Delta$ . Even in the vortex core regions surrounded by circles with a radius of  $\xi$ , however, we could find a smaller gap of 40–50 meV, as can be seen from Fig. 2(d), although the tunneling spectra obtained at the centers of the circles showed typical pseudogaplike features, i.e., a large gap and the suppression of coherence peaks. Figure 3 shows (a) a  $\Delta$  map and (b) the corresponding differential conductance image. Figure 4 is a tunneling spectrum taken at the off-center location marked by a cross in Fig. 3(a), clearly indicating a small  $\Delta \sim 40$  meV with suppressed coherence peaks and in-gap structures at  $\pm 12.5$  meV. Therefore, the present STS results strongly support the second interpretation, namely that the randomly distributed high- $\Delta$  regions effectively pin down the vortices. In the present experiment, such a pinning strength is thought to be comparable with the repulsive electromagnetic interaction

between the vortices, resulting in a significant deformation of the triangular vortex lattice. In this scenario, the vortex arrangement in Bi2212 is determined by the properties of the inhomogeneous electronic distribution, e.g., the size and volume fraction of the pseudogap domains, together with the magnitude of the external magnetic field that regulates the fundamental vortex-vortex spacing.

In summary, we performed STM/STS measurements of Bi2212 single crystals at 4.3 K under 8 T, in order to inves-

tigate the correlation between the vortex distribution and the inhomogeneous electronic distribution. We successfully imaged vortices and the spatial distribution of  $\Delta$ . We found that vortices tend to form a triangular lattice within a short range of  $\sim a_0$ , although the longer range correlation almost completely disappears. Based on the comparison between the vortex distribution and the gap map, we conclude that the vortices are predominantly pinned down in the regions displaying pseudogaps.

- <sup>1</sup>I. Maggio-Aprile, C. Renner, A. Erb, E. Walker, and Ø. Fischer, *Phys. Rev. Lett.* **75**, 2754 (1995).
- <sup>2</sup>K. Shibata, M. Maki, T. Nishizaki, and N. Kobayashi, *Physica C* **392-396**, 323 (2003).
- <sup>3</sup>S. H. Pan, E. W. Hudson, A. K. Gupta, K.-W. Ng, H. Eisaki, S. Uchida, and J. C. Davis, *Phys. Rev. Lett.* **85**, 1536 (2000).
- <sup>4</sup>G. Levy, M. Kugler, A. A. Manuel, Ø. Fischer, and M. Li, *Phys. Rev. Lett.* **95**, 257005 (2005).
- <sup>5</sup>K. Matsuba, H. Sakata, N. Kosugi, H. Nishimori, and N. Nishida, *J. Phys. Soc. Jpn.* **72**, 2153 (2003).
- <sup>6</sup>B. Keimer, W. Y. Shih, R. W. Erwin, J. W. Lynn, F. Dogan, and I. A. Aksay, *Phys. Rev. Lett.* **73**, 3459 (1994).
- <sup>7</sup>C. Renner, B. Revaz, K. Kadowaki, I. Maggio-Aprile, and Ø. Fischer, *Phys. Rev. Lett.* **80**, 3606 (1998).
- <sup>8</sup>B. W. Hoogenboom, K. Kadowaki, B. Revaz, M. Li, C. Renner, and Ø. Fischer, *Phys. Rev. Lett.* **87**, 267001 (2001).
- <sup>9</sup>G. Kinoda, T. Yamanouchi, H. Suzuki, K. Kitazawa, and T. Hasegawa, *Physica C* **353**, 297 (2001).
- <sup>10</sup>G. Kinoda, H. Mashima, K. Shimizu, J. Shimoyama, K. Kishio, and T. Hasegawa, *Phys. Rev. B* **71**, 020502(R) (2005).
- <sup>11</sup>A. Yazdani, C. M. Howald, C. P. Lutz, A. Kapitulnik, and D. M. Eigler, *Phys. Rev. Lett.* **83**, 176 (1999).
- <sup>12</sup>E. W. Hudson, S. H. Pan, A. K. Gupta, K.-W. Ng, and J. C. Davis, *Science* **285**, 88 (1999).
- <sup>13</sup>I. Maggio-Aprile, C. Renner, A. Erb, E. Walker, and Ø. Fischer, *Nature (London)* **390**, 487 (1997).
- <sup>14</sup>S. Nakao, K. Ueno, T. Hanaguri, K. Kitazawa, T. Fujita, Y. Nakayama, T. Motohashi, J. Shimoyama, K. Kishio, and T. Hasegawa, *J. Low Temp. Phys.* **117**, 341 (1999).
- <sup>15</sup>M. Muralidhar, N. Sakai, N. Chikumoto, M. Jirsa, T. Machi, M. Nishiyama, Y. Wu, and M. Murakami, *Phys. Rev. Lett.* **89**, 237001 (2002).
- <sup>16</sup>M. Muralidhar, N. Sakai, M. Nishiyama, M. Jirsa, T. Machi, and M. Murakami, *Appl. Phys. Lett.* **82**, 943 (2003).
- <sup>17</sup>S. Kaneko, Y. Ono, N. Nishida, and T. Kambara, *Surf. Sci.* **493**, 692 (2001).
- <sup>18</sup>S. H. Pan, J. P. O'Neal, R. L. Badzey, C. Chamon, H. Ding, J. R. Engelbrecht, Z. Wang, H. Eisaki, S. Uchida, A. K. Gupta, *et al.*, *Nature (London)* **413**, 282 (2001).
- <sup>19</sup>C. Howald, P. Fournier, and A. Kapitulnik, *Phys. Rev. B* **64**, 100504(R) (2001).
- <sup>20</sup>K. M. Lang, V. Madhavan, J. E. Hoffman, E. W. Hudson, H. Eisaki, S. Uchida, and J. C. Davis, *Nature (London)* **415**, 412 (2002).
- <sup>21</sup>Z. Wang, J. R. Engelbrecht, S. Wang, H. Ding, and S. H. Pan, *Phys. Rev. B* **65**, 064509 (2002).
- <sup>22</sup>G. Kinoda, T. Hasegawa, S. Nakao, T. Hanaguri, K. Kitazawa, K. Shimizu, J. Shimoyama, and K. Kishio, *Phys. Rev. B* **67**, 224509 (2003).
- <sup>23</sup>G. Kinoda, T. Hasegawa, S. Nakao, T. Hanaguri, K. Kitazawa, K. Shimizu, J. Shimoyama, and K. Kishio, *Appl. Phys. Lett.* **83**, 1178 (2003).
- <sup>24</sup>H. Mashima, N. Fukuoka, Y. Matsumoto, G. Kinoda, T. Kondo, H. Ikuta, T. Hitosugi, and T. Hasegawa, *Phys. Rev. B* **73**, 060502(R) (2006).
- <sup>25</sup>Z. Wang, J. R. Engelbrecht, S. Wang, H. Ding, and S. H. Pan, *Phys. Rev. B* **65**, 064509 (2002).
- <sup>26</sup>R. Cubitt, E. M. Forgan, G. Yang, S. L. Lee, D. M. Paul, H. A. Mook, M. Yethiraj, P. H. Kes, T. W. Li, A. A. Menovsky *et al.*, *Nature (London)* **365**, 407 (1993).